Prediction of AVM obliteration after stereotactic radiotherapy using radiobiological modelling

2002 Phys. Med. Biol. 47 2471

(http://iopscience.iop.org/0031-9155/47/14/308)

INSTITUTE OF PHYSICS PUBLISHING PHYSICS IN MEDICINE AND BIOLOGY

Phys. Med. Biol. **47** (2002) 2471–2494 PII: S0031-9155(02)34702-X

Prediction of AVM obliteration after stereotactic radiotherapy using radiobiological modelling

Panayiotis Mavroidis[1], Kyriaki Theodorou[1,2], Dimitrios Lefkopoulos[3], François Nataf[4], Michel Schlienger[5], Bengt Karlsson[6], Ingmar Lax[7], Constantin Kappas[2], Bengt K Lind[1] and Anders Brahme[1]

[1] Department of Medical Radiation Physics, Karolinska Institutet and Stockholm University, Stockholm, Sweden
[2] Department of Medical Physics, Medical School, Thessaly University, Larisa, Greece
[3] Department of Radiation Physics, Tenon Hospital, Paris, France
[4] Department of Neurosurgery, St Anne Hospital, Paris, France
[5] Department of Radiation Oncology, Tenon Hospital, Paris, France
[6] Department of Neurosurgery, Karolinska Hospital, Stockholm, Sweden
[7] Department of Hospital Physics, Radiumhemmet, Karolinska Hospital, Stockholm, Sweden

E-mail: takis@radfys.ks.se (P Mavroidis)

Received 11 March 2002, in final form 20 May 2002
Published 4 July 2002
Online at stacks.iop.org/PMB/47/2471

Abstract

This study was carried out in order to derive the radiobiological parameters of the dose–response relation for the obliteration of arteriovenous malformation (AVM) following single fraction stereotactic radiotherapy. Furthermore, the accuracy by which the linear Poisson model predicts the probability of obliteration and how the haemorrhage history, location and volume of the AVM influence its radiosensitivity are investigated. The study patient material consists of 85 patients who received radiation for AVM therapy. Radiation-induced AVM obliterations were assessed on the basis of post-irradiation angiographies and other radiological findings. For each patient the dose delivered to the clinical target volume and the clinical treatment outcome were available. These data were used in a maximum likelihood analysis to calculate the best estimates of the parameters of the linear Poisson model. The uncertainties of these parameters were also calculated and their individual influence on the dose–response curve was studied. AVM radiosensitivity was assumed to be the same for all the patients. The radiobiological model used was proved suitable for predicting the treatment outcome pattern of the studied patient material. The radiobiological parameters of the model were calculated for different AVM locations, bleeding histories and AVM sizes. The range of parameter variability had considerable effect on the dose–response curve of AVM. The correlation between the dosimetric data and their corresponding clinical effect could be accurately modelled using the linear Poisson model. The derived response parameters can be introduced into the clinical routine with the calculated

accuracy assuming the same methodology in target definition and delineation. The known volume dependence of AVM radiosensitivity was confirmed. Moreover, a trend relating AVM location with its radiosensitivity was observed.

1. Introduction

Obliteration of the arteriovenous malformation (AVM) is the morphological result of a successful treatment using single fraction stereotactic radiotherapy (SRT) (Söderman 2000). The clinical outcome of SRT depends both on the dose delivered to the AVM and its architecture. However, the radiation dose to the AVM nidus is limited by the risk of brain complications (i.e. haemorrhage (it can also be present prior to treatment), epilepsy, neurological deficiencies) (Pollock *et al* 1996, Karlsson *et al* 1997a, 1997b). Most of the centres worldwide use prescription doses that ensure low levels of expected complications (usually less than 3%) being guided by the integrated logistic formula presented by Flickinger and more recently by the relative seriality model (Flickinger 1989, Karlsson *et al* 1997a). These studies suggest that the prescribed dose has to be reduced as the target (nidus) volume increases. Furthermore, it is still not clear to what extent the obliteration of the AVM depends on its volume, its location or a combination of them (Wigg 1999). This is important since the AVM volume can only be modified by embolization prior to radiotherapy. The obliteration rates reported in most of the SRT studies vary between 60% and 90%. In the literature, large AVM materials, which consist of small target volumes (volume of nidus <4 cm^3) following single fraction stereotactic radiotherapy, show a high percentage of totally obliterated malformations with low levels of complications (Merienne *et al* 1991, Lax and Karlsson 1996). However, it is important to mention that in most of the studies lower target doses were applied to the large AVMs to decrease the risk of brain complications (Karlsson *et al* 1997a, 1999).

Single fraction stereotactic radiotherapy is considered to be an effective method of treatment for intracranial AVMs. In particular, it is considered to be the recommended treatment for inoperable or residual cerebral AVMs. SRT differs from conventional radiotherapy in the sense that it employs a single radiation fraction of high dose delivered to a small volume (Colombo *et al* 1994, Lefkopoulos *et al* 1994b, Hladky *et al* 1997). The SRT technique applies very high and localized radiation doses to produce a vascular injury limited to the AVM nidus leading eventually to obliteration while limiting the probability of complications in the surrounding brain tissue (Lefkopoulos *et al* 1994a, Friedman *et al* 1995, Yamamoto *et al* 1995). Nevertheless, there are some centres that apply fractionated treatment using a limited number of fractions. The very heterogeneous dose distribution characterizing SRT and the difficulties of defining the AVM nidus and classifying the neurological symptoms as complication endpoints restrained the construction of models that would accurately predict the obliteration probability and the risk of inducing certain complications.

Embolization and microsurgery are two alternative modalities for treating AVMs. Very often the application of microsurgical resection is constrained due to AVM location or poor patient condition. Furthermore, the demand for a pre-treatment clinical outcome prediction is difficult to be satisfied for embolization and microsurgery since their results are not reproducible (Sisti *et al* 1993, Tew *et al* 1995, Karlsson *et al* 1999). This is because the skills of the physician are of decisive importance for the success of those treatments. These limitations do not hold for SRT since it can be applied independent of the AVM location and the delivered dose can be reproduced very accurately. This is a prerequisite for a close prediction of the treatment outcome. A quantification of the probability for obliteration before treatment

is therefore possible to be obtained (Schwartz *et al* 1997, Pollock *et al* 1998). However, more clinical factors are needed to take into account the inter-patient variability of radiosensitivity.

There are several reports in the literature referring to physical optimization of the AVM treatment (Karlsson 1996, Söderman 2000). However, it is only recently that researchers started studying the radiobiological nature of the AVMs, which leads to their obliteration (Karlsson 1996, Wigg 1999). Models that describe and quantify the biological effect of radiation on tumours and normal tissues have been discussed for more than three decades (Schultheiss *et al* 1983, Withers *et al* 1988, Emami *et al* 1991, Källman *et al* 1992, Ågren 1995, Brahme 1995, Lind *et al* 1999, Mavroidis *et al* 2000). However, their clinical introduction is still very limited. This is because of the lack of accurate clinical data, which prevented the appropriate mathematical formulation of the biophysical and biochemical processes involved in AVM obliteration. This led, mainly at the beginning, to the construction of rather simplified dose–response models, where a number of tissue and patient-specific factors are ignored. In the past, the difficulty in extracting accurate biological data from clinical material stemmed usually from the lack of accurate 3D dose information as well as well-defined follow-up records (Brahme 1997). Furthermore, organ motion in fractionated non-stereotactic treatments and target definition methods in general imposed significant problems in treatment standardization. SRT differs from conventional radiotherapy in the sense that the dose planning preceding the treatment has for more than ten years been three-dimensional and that a very small volume is, in general irradiated. This makes possible the retrieval of accurate dose volume information from existing dose plans and use of them in retrospective analyses.

A number of models that try to predict the probability for obliteration have been published. However, predictions produced by different models are likely to differ since they are usually based on different assumptions and clinical information (Dutreix *et al* 1988, Karlsson *et al* 1999). Therefore, the parameters used in a specific model should be derived from patient materials as similar as possible to those that are intended to be applied because the methodology (target definition, dose range, follow-up recording) can significantly affect the determined parameters (Emami *et al* 1991, Merienne *et al* 1991, Flickinger *et al* 1996, Lax and Karlsson 1996, Hladky *et al* 1997). This has been done at Karolinska hospital where the routine plan evaluation is done using a biological model in conjunction with home-derived parameters (Karlsson *et al* 1997a, 1997c, 1999).

As the AVM volume increases, so does the need for an accurate estimate of the obliteration probability and the risk of complications caused by the planned treatment. This would allow a comparison among the different dose plans that are usually produced during treatment planning aiming at finding the best treatment. Previous work at Karolinska hospital has shown that other parameters such as AVM location and haemorrhage history as well as the risk of late haemorrhage after incomplete obliteration are of importance in defining the optimum dose for AVM treatment in a given patient (Karlsson 1996, Söderman 2000).

The present work deals with a biological model that predicts the obliteration rate in stereotactic radiotherapy of AVM. An important basis for the suggested model is the relation observed between the incidence of obliteration and the dose delivered to the target volume. It is shown that the radiobiological model qualitatively describes this relation, and that the parameters of the model can be determined for a correct quantitative description of the relation.

Different parameters influencing the AVM response are taken into account such as the lesion location, previous haemorrhage and volume. Using the above information a maximum likelihood fitting is performed to the linear Poisson model, which describes the dose–response of the AVM. Radiobiological parameters as well as their confidence limits are estimated. These confidence intervals describe the variation of radiosensitivity among the patients and provide a better description of the expected clinical outcome.

Table 1. Description of the dosimetric and clinical characteristics of the patient population.

Patients	85	Irradiation technique	
Males	52 (61.2%)	Mono-isocentric	55 (64.7%)
Females	33 (38.8%)	Multi-isocentric	30 (35.3%)
		Reference isodose	60–70%
Age		Reference dose (Gy)	
Range	6–68 years	Range	18–28
Mean	33.8 years	Mean	24.3
Median	34 years		
AVM location		Mean dose (Gy)	
Central	35 (41.2%)	Range	16–33
Peripheral	50 (58.8%)	Mean	28.4
AVM volume (cm^3)	0.3–8.8		
Haemorrhage before treatment		Follow-up	
Yes	50 (58.8%)	Angiography	85 (100%)
No	35 (41.2%)	MRI (additional)	51 (60%)
		Obliteration rate	58 (68.2%)
Other symptoms		Obliteration time	
Neurological deficit	6 (7.1%)	Range	6–54 months
Epilepsy	17 (20.0%)	Mean	20.3 months

The analysis is based on an accurate delineation of the AVM outline during the organ-contouring procedure. Information about the dose–response relations of the AVM and brain complications has been reported by many scientists (Karlsson *et al* 1997a, 1999). Newer and more accurate clinical data, such as those presented here, are being published at an increasing rate, making the biological treatment planning evaluation more reliable.

2. Materials and methods

2.1. Study population

This study was based on 85 consecutive patients with angiographically proven AVMs who were treated with single fraction stereotactic radiotherapy from 1990 until 1992 at Tenon Hospital, Paris (Schlienger *et al* 2000). This group was not subjected to any prior treatment (embolization or microsurgery) and had at least 5 years follow-up period. Among the patients, there were 33 females and 52 males. The mean age was 33.8 ± 1.4 years (median 34.0 years; range 6–68 years). The patients presented one or more of the following symptoms before treatment: haemorrhage ($n = 50$), neurological deficit ($n = 6$) and epileptic seizure ($n = 17$). Fifty AVMs were peripheral or supratentorial (left sided, right sided and midline) of which 27 were large (>2 cm^3) and 23 small sized (<2 cm^3). Thirty-five AVMs were central or deeply situated (basal ganglia, and midline) of which 14 were large and 21 small sized. The shape of the targets was characterized as spheroid, ellipsoid or irregular. The characteristics of this group, which are also referring to age and gender are summarized in table 1.

2.2. AVM parameters

The AVMs have been grouped according to their location, volume and to whether they had previous haemorrhage or not. An AVM was defined as central if located in mesencephalon, thalamus, basal ganglion, intra- or para-venticular and in the corpus callosum. All the others

were defined as peripheral. The volumes of the AVMs studied varied between 0.3 and 8.8 cm^3 with a mean value of 3.02 cm^3. The incidence of previous haemorrhage in relation to the patient's age and AVM volume was determined for this group of patients.

2.3. Treatment

A description of the different parts of the irradiation technique applied to the patients of this study follows.

Stereotactic system: The patients included in this study were treated using the SALT irradiation technique (Tenon Hospital, Paris, France) (Betti *et al* 1989, Talairach and Tournoux 1992, Lefkopoulos *et al* 1993, Touboul *et al* 1998). The patients were seated in a Betti armchair. In this technique, patient's head is immobilized using the Talairach stereotactic frame and then the patient sits in a sort of rocking chair with the frame attached to a horizontal rotation axis passing through the isocentre. By moving the chair and the gantry of the linac, the stereotactic irradiation could be delivered in steps of 5 mm covering an angle of 145° in the sagittal plane and 170° in the coronal plane. A GE-CGR Saturne 43 Linear Accelerator with 1 mm isocentre precision for 130° arc has been used for patient irradiation. Furthermore, a set of eight exchangeable circular collimators (diameter of 6 to 20 mm at isocentre (100 cm)) was used to deliver circular 15 MV x-ray minibeams in four to eleven coronal arcs.

AVM nidus definition: SRT treatment planning requires an accurate definition of the true three-dimensional shape and size of the AVM nidus. The stereotactic imaging techniques used in this patient population were computerized tomography, classical and digital angiography and magnetic resonance imaging.

Computerized tomography (CT) yields complete three-dimensional information, but its sensitivity is not sufficient to detect the small blood vessels without contrast injection. Since the contrast dye passes through the brain in a few seconds and most of the CT scanners have a too long scan time to acquire the dynamic image of the cerebral blood vessels, CT images are only used for the three-dimensional head reconstruction (anatomy definition and critical structures location) and for dose calculation.

Angiography is the most common diagnostic modality for AVM delineation but it has substantial limitations because it gives access to only two projected images. There are two kinds of angiographic images, the classical angiography and the digital subtraction angiography (DSA). The first kind is used for target localization since it has minimum distortion and the localization markers can be easily visualized (upper images of figure 1). The second kind is used for better target definition. DSA images are distorted due to the electron-optical characteristics of the x-ray image intensifier so they cannot be directly used for stereotactic target localization (middle right image of figure 1) (Theodorou *et al* 1997, 1999).

Magnetic resonance imaging (MRI) is less invasive than angiography and its visualization results are superior since it gives three-dimensional information about the AVM and the surrounding structures. Nevertheless, MRI images are not usually used for stereotactic target localization due to geometric image distortion (middle left image of figure 1). In stereotactic radiotherapy MRI is used to better assess the shape of the nidus. Furthermore, it allows modification of the treatment volume, particularly exclusion of vulnerable tissues, such as the optic nerves. A volume may be built from angiography and subsequently edited with the aid of MRI. In large AVMs the prescription volume may be edited to minimize the volume actually irradiated. It is, however, very difficult to evaluate the impact of this routine modification on the final outcome. Additionally, MRI is not very useful in assessing the remainder of a newly embolized or operated AVM (Söderman 2000). However, angiography still remains the 'golden standard' particularly for patients previously operated or embolized. In this study,

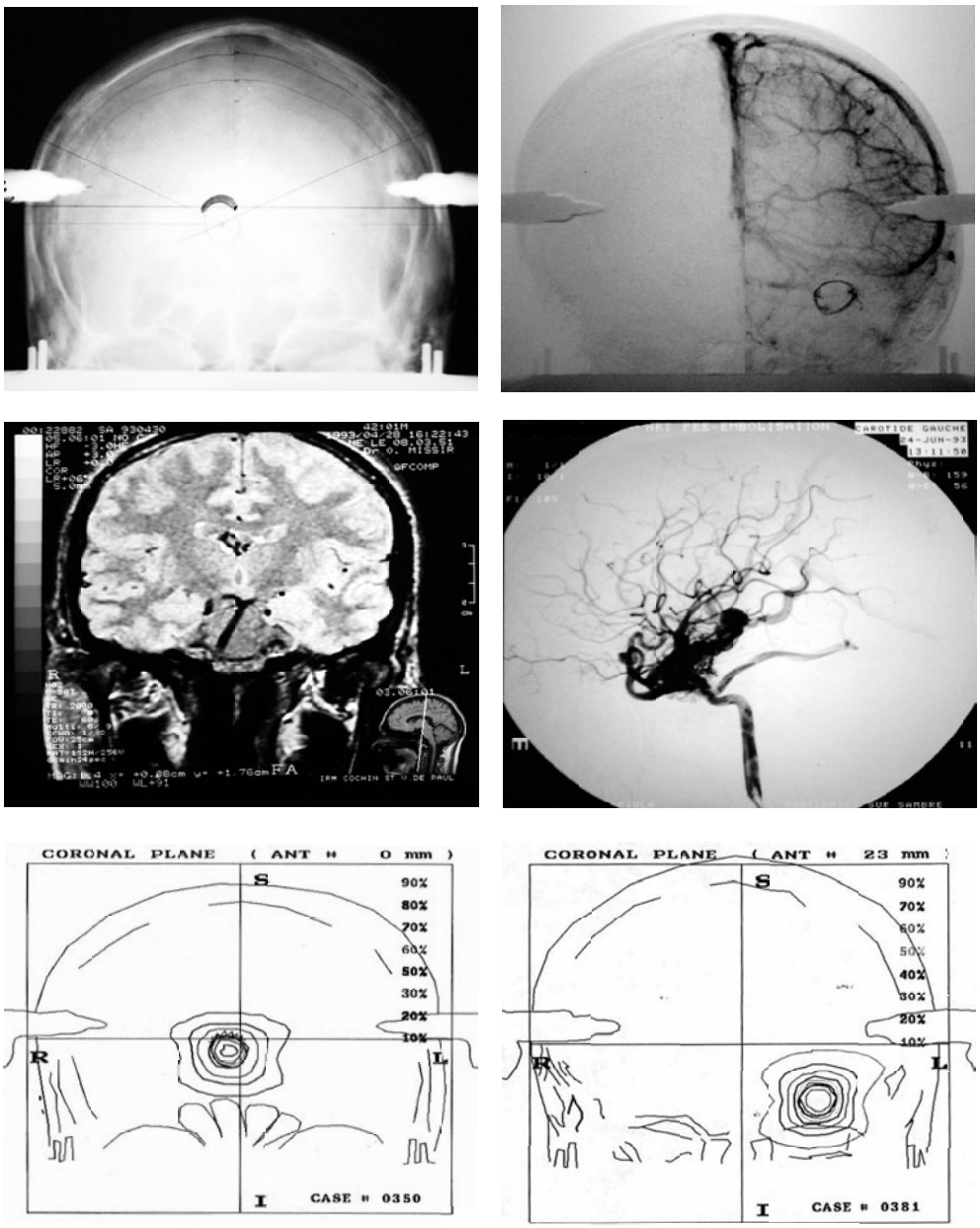

Figure 1. In SRT, treatment planning is strongly dependent on the imaging modalities that are available. In the two panels the coronal images of two AVM patients are shown. The upper coronal images are a classical angiography used for target localization and a subtracted conventional angiography for target delineation. The MRI image (middle left) represents an imaging modality that is used for better target (nidus) visualization. The use of the corresponding DSA image (middle right) also aims at a better target visualization. Finally, the lower two graphs are the corresponding reconstructed coronal images from the TPS at the level of isocentre with the isodose distribution being also demonstrated. The order with which the images are arranged represents the information and process flow in treatment planning.

MRI examination was performed on a large number of patients (60%) in order to assess parenchymal changes.

AVM localization: The AVM nidus was localized using stereotactic stereoscopic angiography films obtained teleradiographically (using distance of 5 m) to limit radiological magnification (factor = 1.045). Delineation of the target was made by including the whole nidus and the venous collectors (i.e. the beginning of the draining veins). The nidus volume was estimated using the 2D angiographic images and calculated as an ovoid-shaped lesion. A Talairach stereotactic atlas was used by the neurosurgeon to define and outline the critical structures lying adjacent to the nidus.

Irradiation technique: The maximum irradiation space was 120° in the antero-posterior (AP) and 130° in the left–right direction whereas the patients were irradiated using 4–11 coronal arcs/per isocentre. Fifty-five (64.7%) of the patients received monoisocentric treatment while the rest were treated with 2–5 isocentres (cf table 1).

Dose prescription: The applied irradiation protocol defined a dose of 24–25 Gy to be delivered to the periphery of the lesion, which should be encompassed by the 60%–70% peripheral reference isodose. In the study group, the reference (isodose) dose varied between 18 and 28 Gy, with a mean value of 24.3 Gy. The mean dose to the target volume ranged between 16 and 33 Gy with an average of 28.4 Gy. In cases of large AVM nidus the dose had to be decreased to avoid complications to the adjacent critical structures. Consequently, the peripheral dose was reduced by 10%–15% and a 60% peripheral reference isodose was used to encompass the nidus. Depending on the lesion size and shape, up to five isocentres were used to satisfy the demands imposed by the irradiation protocol.

Dose calculation: Recent technological developments were used to transmit stereotactic angiography films and CT scans from St Anne Hospital to Tenon through a digital network. In this way the ARTEMIS 3D, which is a treatment planning system (TPS) for stereotactic radiotherapy developed at Tenon Hospital, Paris could be used (Lefkopoulos *et al* 1993). The ARTEMIS 3D is able to carry out both qualitative plan evaluations such as production of isodose charts or dose distribution profiles (lower parts of figure 1), and quantitative evaluations such as dose–volume histograms. CT scan images with slice thickness of 2.5 mm for the entire head were transferred to the ARTEMIS 3D TPS. The dose matrix used for the calculation of the dose distribution delivered to each patient was $100 \times 100 \times 100\,\mathrm{mm}^3$ ($1\,\mathrm{mm}^3$ voxel size). From this dose matrix, which is corrected for eventual tissue inhomogeneities, the corresponding cumulative and differential dose volume histograms (DVHs) of the target, critical structures and normal brain tissue were calculated for treatment plan evaluation. The complete 3D geometry and dose distribution of all patients in the study were used for the determination of the AVM radiobiological parameters.

2.4. Follow-up

Patient follow-up included annual clinical and ophthalmologic examinations, an annual control angiogram and an annual MRI. Post-treatment angiography was performed on all patients of the study. The mean angiographic follow-up was 42.0 ± 2.3 months (median 37.5 months; range 7–117 months). The term 'complete angiographic obliteration' has been used to account for the obliteration rate and it was defined as *normal blood flow*, *complete absence of pathologic vessels at the site of the nidus and normalization of the blood flow in the efferent veins*. The follow-up procedure was based on the registration of the following variables: previous treatment (surgery or incomplete neuroradiological embolization), targeted volume of the nidus, location of the nidus, minimum dose, coverage ratio (CR) and dose at the isodose which encompassed the targeted volume. The minimum dose was defined as the smallest dose

received by parts of the nidus situated beyond the reference peripheral isodose. The CR was defined as the ratio of the nidus volume encompassed by the reference isodose to the total volume of nidus computed from differential DVHs. These data are the result of a more recent calculation, because at the time of treatment, the methodology of quantitative evaluation based on DVHs was not yet in use.

2.5. Radiobiological models

The radiobiological statistical models that have most frequently been used to describe the dose–response relation of AVM are the K index, the Schwartz model, the Flickinger model and the recently introduced Karlsson–Lax model. An intercomparison of these models has already been done (Karlsson *et al* 1999). The radiobiological model that was used throughout this work for calculating dose–response parameters of the AVM is the linear Poisson model (Källman *et al* 1992, Mavroidis *et al* 1997, Lind *et al* 1999). The suitability of the linear Poisson model for describing the dose–response relation of AVM was based on the approach that an AVM generally consists of a large number of arteries ('cells'), which have to be eradicated. So, all the 'cells' of the nidus have to be killed. If better imaging information were available the different arteries could be better viewed and treated separately by the model leading to a better formulation of AVM obliteration. The Karlsson–Lax model was also applied in order to estimate its clinical accuracy.

$$\text{Linear Poisson model} \qquad P(D) = \exp(-\mathrm{e}^{e\gamma-(D/D_{50})(e\gamma-\ln\ln 2)}) \tag{1}$$

where $P(D)$ is the probability of causing AVM obliteration assuming that the nidus is irradiated uniformly with a dose D. D_{50} is the dose which gives a response probability of 50% and γ is the maximum normalized value of the dose–response gradient. The parameters D_{50} and γ characterize the shape of the AVM dose–response relation.

The Karlsson–Lax model assumes that the obliteration probability of AVM can be determined using only the minimum peripheral dose to the nidus, $D_{\min}$.

$$\text{Karlsson–Lax model} \qquad P(D) = a\ln(D_{\min}) - b. \tag{2}$$

The minimum dose used in this formula represents the value of the best-fit isodose curve to the target periphery assuming a total coverage of the AVM nidus. This formula is based on the observation that a logarithmic function describes very closely the empirical relation between the incidence of obliteration and the minimum dose. The values of the fitting parameters a and b published by Karlsson and Lax were 35.69 and 39.66 respectively (Karlsson *et al* 1999). These values were derived from their patient material, which is based on Gamma Knife stereotactic radiotherapy. When those values were applied on the present material the predicted obliteration rate overestimated the actual observation by 6%. For this reason, those parameters have been estimated again using the present patient population. Moreover, the prescribed dose to the reference isodose, which encompasses the target is also used in the Karlsson–Lax model as an approximation of the peripheral dose (although the degree of this approximation depends on the coverage ratio).

For a heterogeneous dose distribution, which is most likely to be applied in practice, the response of AVM using the linear Poisson model is given by the expression

$$P(\vec{D}) = \prod_{i=1}^{M} [P(D_i)]^{\Delta v_i} \tag{3}$$

where $\Delta v_i (= \Delta V_i / V_{\text{ref}})$ is the fractional irradiated subvolume of the AVM compared to the reference volume for which the values of D_{50} and γ have been calculated. $P(D_i)$ is the probability of AVM response when the AVM has the reference volume and is irradiated to

dose D_i as described by equation (1) and M is the total number of voxels or subvolumes in the AVM receiving a certain dose.

The reference volume is related to the characteristics of the clinical material from which the parameters D_{50} and γ were calculated. In this study, the mean volume of the clinical material (3.0 cm^3) was used as the reference volume. The radiation sensitivity was assumed to be homogeneous throughout the AVM volume of each patient.

The biologically effective uniform dose, $\bar{\vec{D}}$, is the uniform dose that causes exactly the same obliteration probability as the real dose distribution delivered to the individual patient (Brahme 1994, Niemierko 1997, Mavroidis *et al* 2000, 2001).

$$\bar{\vec{D}} = D_{50}\frac{\mathrm{e}\gamma - \ln(-\ln(P(\vec{D})))}{\mathrm{e}\gamma - \ln(\ln(2))}. \tag{4}$$

In this work, this concept is used to find for every patient in the study population the uniform dose that is biologically as effective as the dose distribution, $\vec{D}$ delivered to the patient. For each patient the effectiveness of the applied dose distribution is calculated by the linear Poisson model and the estimated radiobiological parameters.

2.6. Maximum likelihood fit of the response model to clinical data

The values of the radiobiological parameters used by the linear Poisson model and their uncertainties were determined through a fit of the theoretical predictions for obliteration (applying the dosimetric information of each patient to the response model) to the clinical follow-up data. For the fitting of the parameters the maximum likelihood method was used, which determines the best estimates of the parameters by maximizing the likelihood to reproduce the given pattern of observations. The chosen biological model for estimating the obliteration probability, P_{obl} consists of two sets of parameters. One set is usually model dependent and is denoted here by the vector $\vec{X}$ whereas the other set, which is treatment dependent, is denoted by the vector $\vec{\theta}$. In the present case, $\vec{X} = \{D_{50}, \gamma\}$ and $\vec{\theta} = \{\vec{D}, \vec{V}\}$. The likelihood function is composed of two separate terms. The first term corresponds to the patients that had obliteration because of the treatment while the second term corresponds to the patients whose AVMs did not obliterate. The likelihood function L, is then defined as follows:

$$\begin{aligned} L(\vec{X} \mid \vec{\theta}) &= L((D_{50}, \gamma), (\vec{D}, \vec{V})) \\ &= \prod_{i=1}^{m} P_{\mathrm{obl}}((D_{50}, \gamma), (\vec{D}_i, \vec{V}_i)) \times \prod_{j=1}^{n} (1 - P_{\mathrm{obl}}((D_{50}, \gamma), (\vec{D}_j, \vec{V}_j))) \end{aligned} \tag{5}$$

where the indices m and n run over the patients with and without AVM obliteration respectively. For simplicity, the calculations were performed using the logarithm of the likelihood function, $\ln L$ (or $\log L$):

$$\begin{aligned} &\ln L((D_{50}, \gamma), (\vec{D}, \vec{V})) \\ &\quad= \sum_{i=1}^{m} \ln(P_{\mathrm{obl}}((D_{50}, \gamma), (\vec{D}_i, \vec{V}_i))) + \sum_{j=1}^{n} \ln(1 - P_{\mathrm{obl}}((D_{50}, \gamma), (\vec{D}_j, \vec{V}_j))) \\ &\quad= \sum_{i=1}^{m} \ln\left(\prod_{k=1}^{M_i}\left(\exp\left(-\mathrm{e}^{\mathrm{e}\gamma-(D_{ik}/D_{50})(\mathrm{e}\gamma-\ln(\ln(2)))}\right)\right)^{V_{ik}}\right) \\ &\qquad+ \sum_{j=1}^{n} \ln\left(1 - \prod_{k=1}^{M_j}\left(\exp\left(-\mathrm{e}^{\mathrm{e}\gamma-(D_{jk}/D_{50})(\mathrm{e}\gamma-\ln(\ln(2)))}\right)\right)^{V_{jk}}\right). \end{aligned} \tag{6}$$

In practice, equations (5) and (6) represent the probability with which the biological model describes the observed pattern of obliterations. In our case, it gives the likelihood that the group of the $m + n$ patients has the observed AVM obliteration rate. The best estimates of the parameters of the likelihood function (the components of the vector $\vec{X}$), are those that maximize the likelihood function.

A minimization package (MINOS) (Murtagh and Saunders 1995) together with an in-house developed code were used to find the values of the model parameters that maximize the likelihood function. The parameter space that was used during the calculations was unrestricted. The global maximum was reached through starting point iterations covering a large range of the initial values to avoid possible local maxima. An evaluation of the parameter errors was made by calculating the 68% and 95% confidence intervals (Schilstra and Meertens 2001). The variance–covariance matrix is usually used to determine the confidence interval of the model parameters assuming that the errors of the estimated parameters are normally distributed. In such a case, the individual confidence regions are given by the square root of the diagonal elements of this matrix. However, for non-normal or pathological likelihood functions one should search numerically to find the confidence regions of the parameters, which are determined by the intersection of the hyper-surface $\ln L(\vec{X} \mid \vec{\theta})$ with the $\ln L = \ln L_{\max} - \frac{1}{2}\chi_a^2(k)$ plane, where k is the number of dimensions of the likelihood function. The region $[\vec{X}_{\min}, \vec{X}_{\max}]$ derived with this procedure is then treated as a confidence region of probability content a. Usually, the probability a corresponds to the confidence regions of 68% or 95%. In order to study the impact of the parameter uncertainties on the dose–response relation, an envelope of dose–response curves was calculated using the derived parameter values. The described procedure represents a first step in quantifying the confidence interval of the dose–response curve, due to the uncertainties in D_{50} and γ parameters.

2.7. Goodness of fit

The goodness of fit was estimated for both the Poisson and the Karlsson–Lax models by two independent methods. First, according to the method described by Jackson *et al* 1995 (see also Eadie *et al* 1971): given D_{50} and γ from the maximization, the average of the likelihood function and its variance were calculated assuming Gaussian distribution for the likelihood function. The expected mean value and standard deviation were then compared to the likelihood function value observed in the maximization and second, by performing chi-square tests to grouped patient data.

The goodness of fit can be estimated by comparing the clinical observations against the theoretical predictions. For this purpose, the histograms of the clinical results and the corresponding theoretical predictions, which were calculated using the dose distribution delivered to each patient, were formed. Calculating the obliteration probability for each patient using the best estimates of the model parameters $\hat{P}^i_{\text{obl}} = P^i_{\text{obl}}(\hat{\vec{X}} \mid \vec{\theta}_i)$ and averaging over all patients, the mean value of L can be calculated as follows:

$$\bar{L} = \sum_{i=1}^{m+n} \left[\left(1 - \hat{P}^i_{\text{obl}}\right) \ln \left(1 - \hat{P}^i_{\text{obl}}\right) + \hat{P}^i_{\text{obl}} \ln \left(\hat{P}^i_{\text{obl}}\right) \right] \tag{7}$$

and the variance, V_L is then given by

$$V_L = \sum_{i=1}^{m+n} \left[\hat{P}^i_{\text{obl}} \left(1 - \hat{P}^i_{\text{obl}}\right) \left(\ln \left(\frac{\hat{P}^i_{\text{obl}}}{1 - \hat{P}^i_{\text{obl}}} \right) \right)^2 \right]. \tag{8}$$

Assuming that the value of L is normally distributed, equations (7) and (8) can be used to estimate the goodness of fit of the maximum likelihood method.

In the second method, the predicted obliteration probability for each patient was calculated using the fitted model parameters. Subsequently, the patients were ordered with respect to the predicted obliteration probabilities and grouped into bins of the obliteration rate (OR) (bin width: 0.1). Then, the agreement between predicted and observed obliteration rates in each group was determined by calculating a chi-square test (defined as the sum of the squares of the differences between the observed and the average values of the predicted ORs in each group weighted with the inverse of the square errors on the data points deduced from binomial statistics) (cf figure 6). The same test was also performed using the obliteration predictions and clinical outcomes of the individual patients without applying any grouping.

$$\chi^2 = \sum_{i=1}^{N} \left[\frac{\left(\mathrm{OR}_i - P_i^{\mathrm{obl}}((D_{50}, \gamma), (\vec{D}_i, \vec{V}_i)) \right)^2}{P_i^{\mathrm{obl}}((D_{50}, \gamma), (\vec{D}_i, \vec{V}_i)) \left[1 - P_i^{\mathrm{obl}}((D_{50}, \gamma), (\vec{D}_i, \vec{V}_i)) \right]} \right] \tag{9}$$

where N is the number of data pairs compared. The values of the reduced chi-square $\chi_v^2 = \chi^2/v$ and the probability $P = P_\chi(\chi^2, v)$ of exceeding χ^2 were then calculated.

3. Results

It is evident that the progress of AVM obliteration is influenced by a number of parameters such as the dose to the nidus, the volume, the location and possibly the patient's age. Most of these factors have been taken into account in the estimation of the obliteration probability using biological models. Figure 2(a) shows very clearly the relations between the AVM volume and the dose (mean, prescribed and minimum) against the treatment outcome (i.e. obliteration rate). It is apparent that as the volume of the AVM increases, the obliteration rate decreases while the dose to the target remains almost the same up to 4 cm^3 volume. For larger volumes the dose also decreases with different rates for the different dose quantities as a result of the large dose distribution inhomogeneities. This behaviour indicates that there is a volume effect characterizing the AVM stereotactic irradiation, i.e. larger volumes need a higher dose to obliterate.

Among the symptoms reported before treatment, haemorrhage has been considered as the most important since it has been suggested that it influences the complication rates. However, it has not been investigated if the presence of bleeding influences the radiosensitivity of AVM.

The relationships between age, AVM volume and location against the risk for haemorrhage were assessed through cumulative incidence rate diagrams. In figure 2(b) the annual risk of haemorrhage as a function of location is illustrated. Using the annual risk values shown in the diagram, the expected age distribution at initial haemorrhage in a large patient material can be estimated. On the age axis, the time (years) before the initial haemorrhage for the corresponding groups of patients was used. It was assumed that AVMs are congenital and thus the time at risk was equal to the age of the patient at the time of the initial haemorrhage. The cumulative incidence rate method was obtained by summing up the annual age-specific incidences for each year in the defined age interval. It is clear that the centrally located AVMs are more prone to bleeding than the peripheral AVMs in the whole age range. Figure 2(c) shows the risk of haemorrhage as a function of AVM volume and location. The higher risk for haemorrhage of the central against the peripheral AVMs is also evident and is even more pronounced in the whole volume range. From those two diagrams it is obvious that the risk of haemorrhage increases with age and volume. The rate of increase seems to be age dependent though it appears to be high for small volumes and to gradually saturate towards large AVM volumes. Furthermore, it is apparent that AVM location has a significant effect on the risk

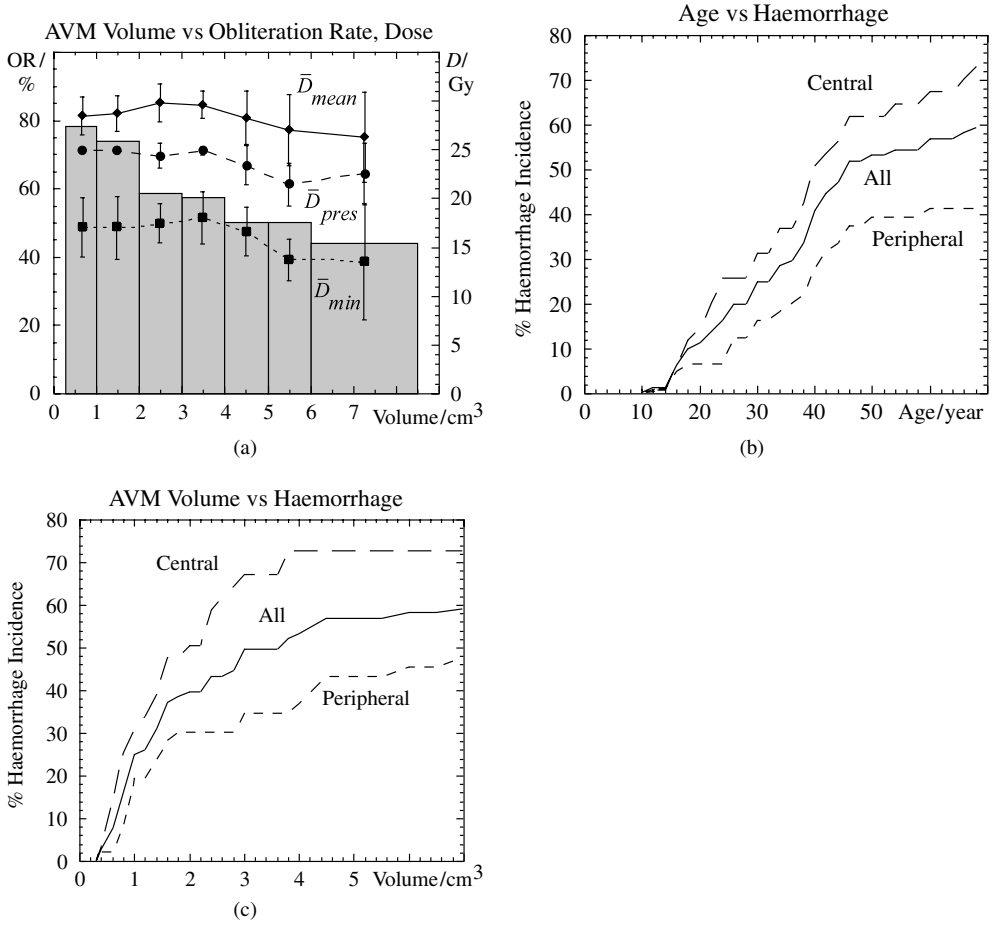

Figure 2. (a) The relations between obliteration rate, AVM size (volume) and dose as they were derived from the clinical material. There is an apparent decrease of the obliteration rate (shaded histogram) as the volume of the AVM increases. Up to the volume of 4 cm^3 the average values of the mean dose, the prescribed dose and the minimum dose to the AVMs remain approximately constant. In larger volumes, all those doses decrease with different rates. This is because the applied protocol tends to deliver lower doses to large AVMs to avoid brain complications. The fact that large AVMs receiving the same dose as similar small AVMs show lower obliteration rates constitutes an indication that larger AVMs may need a higher dose to obliterate than the small AVMs. (b) The annual risk of haemorrhage and its relation to the AVM location. It can be noticed that centrally located AVMs bear a higher risk of eruption than the peripheral AVMs. It is also evident that the increase rate of the risk is age dependent. (c) The incidence of haemorrhage against the AVM volume and location. The AVM location seems to have the same influence on the risk for bleeding as in the annual risk diagram. The rate of increase of the risk is much larger at the small volumes and it saturates towards the large AVMs.

for haemorrhage with centrally located malformations being more prone to rupture than the corresponding peripheral malformations.

The absolute obliteration rate for this group of patients was 68.2% (58 out of the 85 patients considered) and the mean obliteration time was 20.3 months (varied between 6 and 54 months). The estimated time at which complete obliteration took place was considered to be the midpoint between the last angiography showing incomplete obliteration and the

angiography showing complete obliteration. The mean age of the patients at radiotherapy time was found to be 32.9 ± 13.9 years (median 33.0 years) in the obliterated group versus 34.3 ± 17.6 years (median 33.5 years) in the group without obliteration. This indicates that age does not affect the AVM radiosensitivity significantly (it is also necessary to consider the dose to make the statement stronger). The best estimates of the parameters obtained when all the patients were grouped together were $D_{50} = 22.9$ Gy and $\gamma = 1.25$ for a reference volume of $V_{\mathrm{ref}} = 3.0\,\mathrm{cm}^3$. From the normalized individual differential dose–volume histograms of the patient AVMs (the fractional subvolumes of the differential DVH were divided with the AVM volume for every patient separately) the mean differential DVHs were obtained, which are representative of the dose distributions delivered to the patients. This is illustrated in figure 3(a) where different curves are plotted for the group of patients that developed obliteration and the group with incomplete obliteration of the AVM nidus. The obliterated group received higher mean and integral dose than the non-obliterated group. The difference between the two groups becomes larger when looking at the minimum dose. The statistical significance of the difference in dose between the two groups is expressed by the determined dose-response relation for AVM obliteration.

In table 2, the best estimates of the parameters D_{50} and γ for the different patient subgroups are given together with their 68% and 95% confidence regions. The uncertainties of the model parameters were obtained by calculating the hyper-surface of the log-likelihood space for the probabilities given in figure 3(b). These uncertainties stem not only from potential deviations between the calculated and the actually delivered dose to each patient, but mainly from the radiosensitivity variation among the patients included in the study population, inaccurate target definitions and architectural differences between AVMs. So, the dose–response curve of an individual patient should lie within the limits defined by the maximum, minimum and combined values of the D_{50} and γ parameters. This is illustrated in figure 3(c) where the thick line envelope represents the range that the dose–response curve of an individual may be confined to with a probability of 68%. The choice of deriving the confidence interval of a dose–response curve from the D_{50}–γ joint confidence region was based on the consideration that any combination of the parameter values within this region can be possible for a patient.

The maximum likelihood fitting did not show any dependence on the parameter limits chosen for the calculation. In figures 4(a) and 5(a) the mean differential DVHs of the individual subgroups are illustrated. According to these diagrams the central and peripheral AVMs receive similar doses though the group of patients with haemorrhage receives higher doses than the haemorrhage-free group. The dose characteristics of the haemorrhage subgroups can also be seen between the large and the small AVMs where the large AVMs receive lower doses than the small AVMs. These dosimetric characteristics are described quantitatively in figures 4(b) and 5(b) where the average mean and minimum doses of the different patient subgroups are given together with their relative uncertainties.

The radiobiological parameters of the different patient subgroups are shown in table 2. In figures 4(c) and 5(c) the dose–response curves characterized by these parameters are drawn. It is seen that the centrally located AVMs appear to be more radiosensitive than the peripheral AVMs whereas haemorrhage seems to play no important role in radiation-induced obliteration. Furthermore, it seems that radiosensitivity reduces gradually as the AVM volume increases, which supports the argument that larger AVMs need higher doses to obliterate.

The mean and standard deviation of the maximum likelihood function were used to estimate the goodness of fit in every case. The best estimates of the fitted model parameters were used to calculate the individual patient obliteration probabilities. By using these

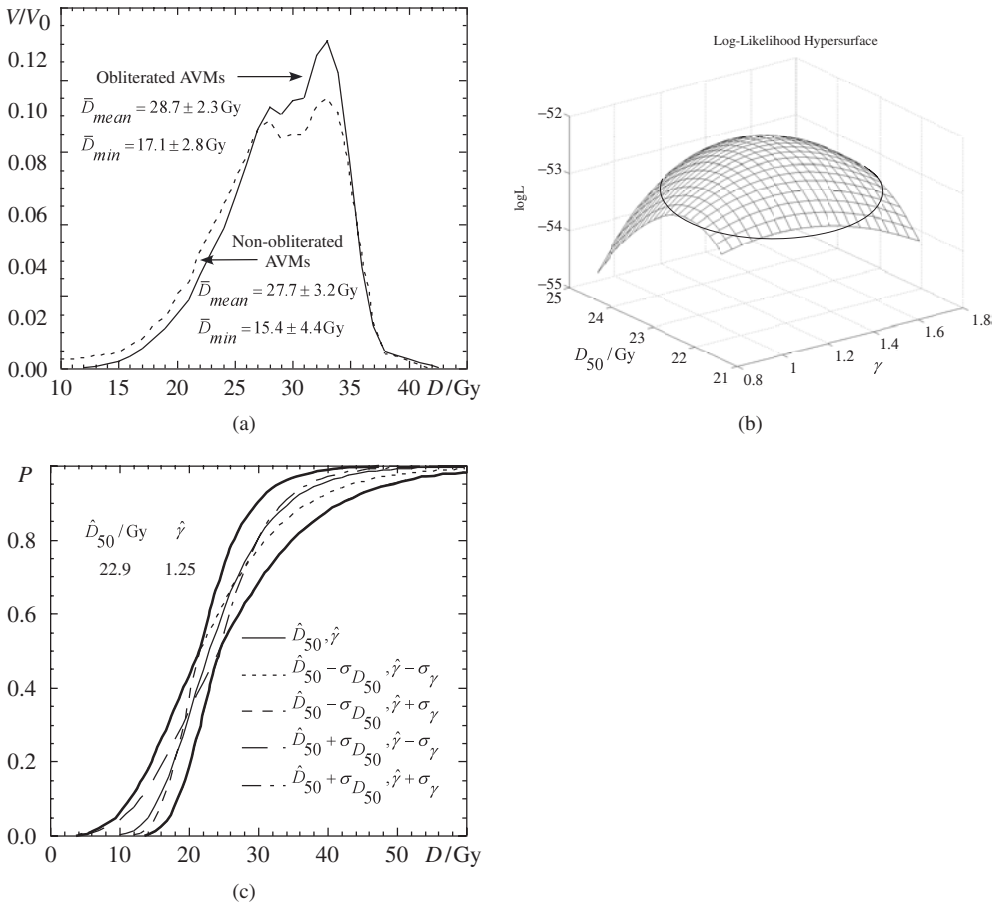

Figure 3. (a) The mean differential dose–volume histograms of the patients with and without complete AVM obliteration. V/V_0 is the fractional volume of the AVM. It is apparent that the obliterated AVMs received a higher integral dose as compared to the non-obliterated ones. The mean and minimum doses of the two patient groups are also provided. (b) The hyper-surface of the log-likelihood space, which was used to calculate the uncertainties of the model parameters (D_{50} and γ). The solid line represents the iso-surface that corresponds to the 68% probability of deviation from the maximum value of the likelihood. The 95% confidence interval was also calculated. (c) The best estimate of the dose–response curve of the AVM (thin solid line) is shown together with its 68% confidence interval (defined by the thick solid lines). This range constitutes the confidence interval of the AVM survival curve representing mainly the variation of inter-patient radiosensitivity.

probabilities, the expected values of the log-likelihood function were calculated for the different patient subgroups. These values were compared with the observed values of the log-likelihood function from the corresponding fits. By assuming a Gaussian distribution of the log-likelihood function, the probability of having a worse fit with the calculated deviation was estimated using the normal error distribution table. For the different subgroups of the linear Poisson model the probability of a worse fit ranges between 60.1% and 66.7% indicating that the model fits well the clinical data in all cases (cf table 3). In the case of the Karlsson–Lax approaches the goodness of fit values (60.1%, 60.2%) are a bit worse than those of the linear

Table 2. Best estimates and confidence intervals of the radiobiological parameters that describe the AVM dose–response. The sets of parameters were derived from the different patient subgroups and biological models.

Patient subgroup	D_{50}	Confidence intervals on D_{50}	γ	Confidence intervals on γ
All AVMs ($V_{ref} = 3.0$ cm^3) (85 patients)	22.9	68%: 21.5−24.3 Gy 95%: 20.6−24.6 Gy	1.25	68%: 0.87−1.66 95%: 0.69−1.87
Peripheral AVMs (50 patients)	24.2	68%: 21.6−26.6 Gy 95%: 20.0−35.1 Gy	0.86	68%: 0.34−1.42 95%: lim.−1.76
Central AVMs (35 patients)	20.9	68%: 18.8−22.4 Gy 95%: 17.3−23.0 Gy	1.91	68%: 1.17−2.83 95%: 0.96−3.34
Large AVMs (>2 cm^3) (41 patients)	24.6	68%: 19.7−27.3 Gy 95%: 15.4−30.2 Gy	0.67	68%: lim.−1.28 95%: lim.−1.64
Small AVMs (<2 cm^3) (44 patients)	19.7	68%: 15.8−22.2 Gy 95%: 12.8−23.1 Gy	1.37	68%: 0.82−2.26 95%: 0.69−2.71
Large AVMs (>4 cm^3) (22 patients)	23.7	68%: 20.4−26.8 Gy 95%: 15.4−30.2 Gy	0.93	68%: 0.09−1.63 95%: lim.−2.05
Small AVMs (<4 cm^3) (63 patients)	22.7	68%: 20.2−24.2 Gy 95%: 18.7−24.9 Gy	1.34	68%: 0.87−2.01 95%: 0.67−2.35
AVMs with haemorrhage (51 patients)	23.3	68%: 21.5−24.7 Gy 95%: 19.8−25.7 Gy	1.62	68%: 0.97−2.35 95%: 0.73−2.67
AVMs without haemorrhage (34 patients)	22.7	68%: 19.7−25.4 Gy 95%: 18.1−27.7 Gy	0.91	68%: 0.41−1.49 95%: 0.14−1.79

	Karlsson–Lax approach			
	a		*b*	
All AVMs (prescribed dose)	62.28	68%: 21.80−102.76	130.42	68%: lim.−277.15
All AVMs (minimum dose)	52.07	68%: 26.68−77.45	75.84	68%: 1.90−149.79

Poisson model. Furthermore, by using chi-square statistics, another estimation of the goodness of fit was obtained for each case. Using the best estimates of the model parameters and the dose distribution to each patient the corresponding obliteration probabilities were calculated. These probabilities were compared to the clinical outcome through the chi-square test for every case and model. In table 3, it is seen that the closest association between the predicted and observed results, is achieved by the linear Poisson model for the whole patient population (probability: 0.91). For the Karlsson–Lax model the results indicate a fit at the border of acceptance (probability: 0.39).

The clinical use of the calculated parameters is illustrated in figure 6. Using the derived radiobiological parameters of the linear Poisson model for the case of the whole population, the dose–response curve of the AVM is calculated for a range of uniform doses. Subsequently, the response probability is calculated for every patient using again those parameters and the dose distribution delivered to the AVM. By applying the concept of biologically effective uniform dose to these probabilities, the corresponding $\bar{\bar{D}}$ values are found. Plotting these dose–response points on the existing diagram they will, by definition, fall exactly on the theoretical dose–response curve. For the Karlsson–Lax model the same course of action was taken using the minimum dose to the AVM instead. In the figure, the chi-square test values differ from those in table 3. This is because in the former case the test is the result of the histogram comparisons shown in the figure though in the latter

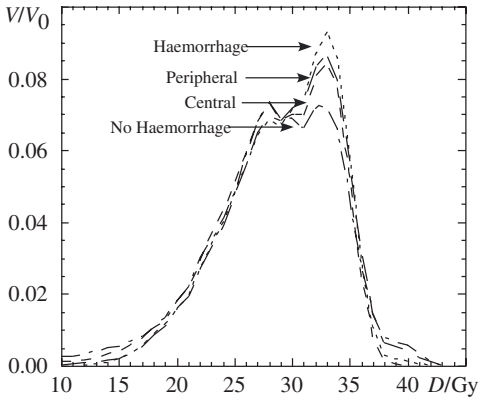

(a)

Subgroups	$\bar{D}_{mean}$	$\sigma_{D_{mean}}/\bar{D}_{mean}$	$\bar{D}_{min}$	$\sigma_{D_{min}}/\bar{D}_{min}$
Peripheral	28.7	0.08	16.7	0.19
Central	27.9	0.11	16.4	0.22
Haemorrhage	28.7	0.07	17.2	0.17
No Haemorrhage	27.9	0.12	15.5	0.26

(b)

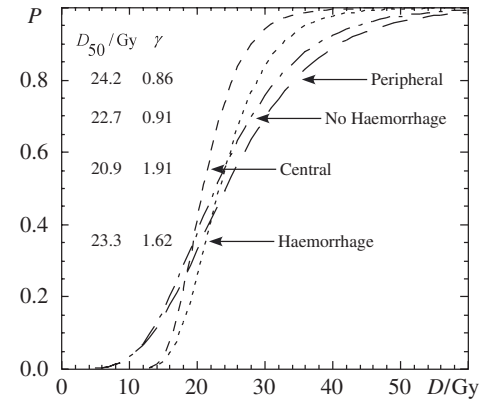

(c)

Figure 4. (a) The mean differential dose–volume histograms of the patients, grouped according to the AVM location and their haemorrhage history. It is shown that the peripheral and central AVMs received similar doses whereas those with haemorrhage received higher doses than those without previous bleeding. The difference in dose of the AVMs with a different haemorrhage history stems mainly from the different proportions of large and small AVMs comprising them. That is because the irradiation protocol applied does not differentiate AVMs by their location or haemorrhage history but only by their size. (b) The mean and minimum doses together with their relative uncertainties are given for the different patient subgroups. (c) The dose–response curves and the corresponding radiobiological parameters of the different patient subgroups are illustrated. The curves indicate that the central AVMs are more radiosensitive than the peripheral AVMs whereas haemorrhage does not seem to influence significantly this factor.

case the comparison between the theoretical predictions and the clinical results is carried out for every patient separately. To examine whether the theoretical curve reproduces the observed obliteration rates it is enough to compare these values for the region around the prescribed dose used by the centre where the patients were treated. If the two values are close enough then the parameters can be used for predicting the obliteration rate for the technique applied. This is a simple way to examine if a set of parameters is compatible with the clinical practice that a centre uses with the prerequisite that the same target definition is used.

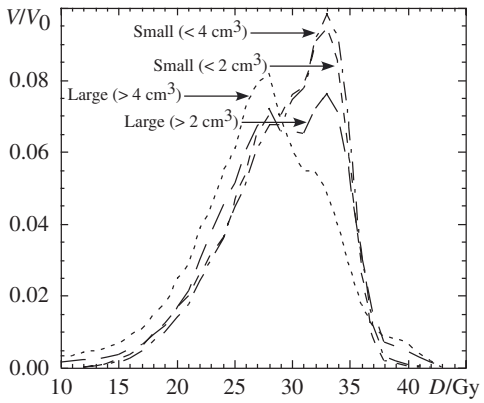

(a)

Subgroups	$\bar{D}_{mean}$	$\sigma_{D_{mean}}/\bar{D}_{mean}$	$\bar{D}_{min}$	$\sigma_{D_{min}}/\bar{D}_{min}$
Large (>2 cm^3)	28.2	0.12	16.1	0.23
Small (<2 cm^3)	28.6	0.06	17.0	0.18
Large (>4 cm^3)	26.7	0.13	14.7	0.29
Small (<4 cm^3)	29.0	0.06	17.2	0.17

(b)

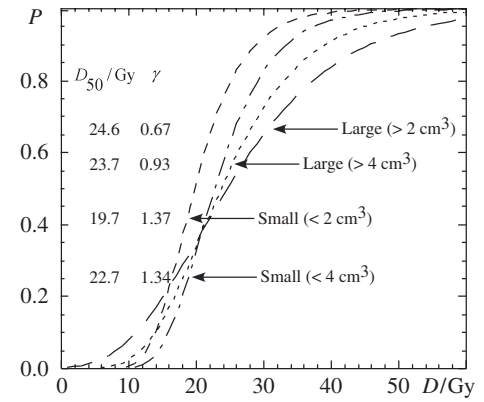

(c)

Figure 5. (a) The mean differential dose–volume histograms of the patients, grouped according to their AVM sizes. It is shown that the small AVMs receive higher doses than the large AVMs. Furthermore, the selection of the cut-off point (in the region 2–4 cm^3) separating AVMs into large and small does not change significantly the dose characteristics of the patient subgroups. The difference in the dose of AVMs with different sizes is due to the irradiation protocols followed to avoid high risk of brain complications. (b) The mean and minimum doses together with their relative uncertainties are given for the different patient subgroups. (c) The dose–response curves and the corresponding radiobiological parameters of the different patient subgroups are illustrated. The response curves demonstrate the gradual change in radiosensitivity imposed by the increase of AVM volume.

4. Discussion

Radiobiological modelling is based on the knowledge and mathematical expression of the biological mechanisms that are responsible for the clinical radiation effect (obliteration in this case). However, the treatment outcome is also dependent on the irradiation methodology or protocol applied. In the radiation treatment of AVM there are two approaches mainly followed in the clinic. The first, aims at delivering a high uniform dose to the whole AVM volume while the second focuses on the peripheral dose covering the nidus. The first irradiation approach assumes that every part of the AVM nidus has to be irradiated to a high dose in order to bring about complete obliteration. This is based on the argument that an AVM generally consists of a large number of arteries, which have to be eradicated. The linear Poisson model benefits

Table 3. Results from the fits of the different biological models on the patient data. The goodness of fit was determined for the different patient subgroups by different methods (Pearson's test, normal error distribution).

Patient subgroup	Predicted OR (%)	Observed OR (%)	$\chi_v^{2\,a}$	$P_\chi\left(\chi_v^2, \nu\right)$	Observed log L	Expected log L	Variance log L	$P_{\text{Worse fit}}$ (%)
All AVMs (85 patients)	66.1	68.2	0.799	0.91	−52.27	−50.59	13.14	64.1
Peripheral AVMs (50 patients)	60.2	62.0	1.089	0.31	−33.07	−32.50	3.90	61.7
Central AVMs (35 patients)	76.3	77.1	1.029	0.42	−16.77	−16.27	9.97	60.6
Large AVMs (>2 cm^3) (41 patients)	57.0	56.1	1.061	0.37	−26.63	−27.67	3.02	66.7
Small AVMs (<2 cm^3) (44 patients)	78.8	79.5	1.118	0.28	−22.44	−21.99	12.72	60.4
Large AVMs (>4 cm^3) (22 patients)	55.4	54.5	1.112	0.33	−13.49	−13.47	2.62	60.1
Small AVMs (<4 cm^3) (63 patients)	70.5	73.0	1.132	0.23	−38.54	−37.07	11.12	63.8
AVMs with Haemorrhage (51 patients)	68.3	70.6	1.092	0.31	−30.97	−30.37	8.23	61.0
AVMs without Haemorrhage (34 patients)	62.3	70.6	0.949	0.55	−17.52	−16.85	4.18	62.2
			Karlsson–Lax Approach					
All AVMs (prescribed dose)	68.1	68.2	1.034	0.39	−52.55	−52.78	11.24	60.2
[b]All AVMs (minimum dose)	69.1	70.0	1.038	0.39	−46.24	−46.08	14.38	60.1

[a] Degrees of freedom = number of patients in the subgroup − number of fitted parameters (=2) −1.
[b] The minimum dose in five of the AVM cases was not available.

dose distributions that deliver high uniform doses to the AVM nidus. The latter approach, which is adopted by the Karlsson–Lax model assumes that the peripheral dose may be the decisive factor in the obliteration of the nidus. This is based on the assumption that only the feeding arteries and the drainage veins of the nidus need to be eradicated for the AVM to obliterate. Many studies in the literature try to associate the minimum dose to the nidus with the obliteration rate to derive the corresponding dose–response relation. The minimum dose may be close to the peripheral dose but it is not the same. It would be much more correct to apply the dose–volume histogram of the peripheral nidus on the linear Poisson model to derive the dose obliteration curve. In this way the significance of the minimum peripheral dose could be validated.

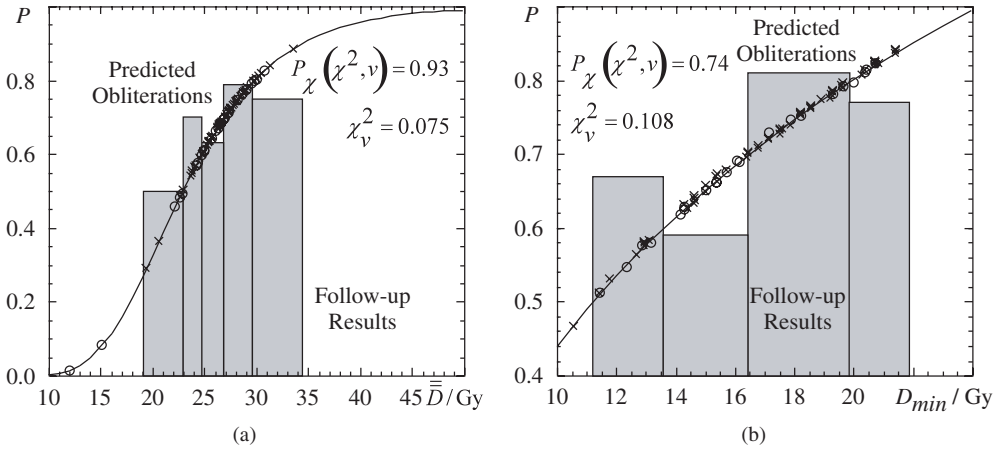

Figure 6. (a) The dose–response curve derived using the linear Poisson model and the radiobiological parameters calculated from the whole patient material. On the same diagram the points of the obliteration probability of each patient have been drawn. These points were calculated using the individual dose distribution delivered to each patient and the model parameters that were calculated. The crosses and the open circles correspond to the patients with and without complete AVM obliteration respectively. The biologically effective uniform dose was used as the unit of the dose axis. (b) The dose–response curve derived using the Karlsson–Lax model and the radiobiological parameters calculated from the patient material. On the same diagram the points of the obliteration probability of each patient have been drawn. These points were calculated using the minimum peripheral dose of the individual dose distribution delivered to each patient and the model parameters that were calculated. The chi-square tests that were applied on a large sample of the patients show that the linear Poisson model predicts closely the clinical results to an extent that is acceptable for clinical use.

Since the derivation of the radiobiological parameters is influenced by both the irradiation protocol applied and the assumptions that the biological model makes, the calculated parameters would be more accurate for clinical materials and techniques similar to those used during the study. Using the estimated values of the biological parameters of the linear Poisson model, the obliteration probability can be calculated as a function of dose for any patient receiving single fraction stereotactic radiotherapy treatment. The confidence intervals of D_{50} and γ are important in order for these parameters to be used in clinical practice.

The target definition is a very significant factor in the estimation of AVM response. The currently applied imaging techniques are not sufficient to estimate accurately the volume of AVM (the deviation between the real and the calculated volume can be of the order of 30%) (Söderman 2000). In some cases, it can be difficult even to decide what to include in the AVM volume. So, the accuracy of the calculated dose–response relations of AVM from different studies is subjected to these uncertainties. The intra-observer target definition variation is generally smaller than that of the inter-observer and both of them are generally much smaller than that of the inter-institutional target definition variation. This is because different institutes generally use different imaging modalities and treatment methodologies.

In this study, the role of the imaging techniques used and the method of delineating the AVM nidus is very important. Studies that use a combination of imaging techniques leading to a delineation of the nidus that is very close to its real volume, are expected to have a closer association of their predictive results with the clinical outcome than studies, which use more conventional delineation methods. Whatever the case might be, the calculated radiobiological parameters from a clinical study are applicable only for the radiotherapy

centres that apply a very similar nidus definition and delineation technique (using similar technological capabilities).

The treatment configurations described in the present study result in a large part of the nidus volume being irradiated to a high dose. Generally, it is desirable to have many different irradiation protocols in the study material because this usually implies that the clinical data cover a large dose range on the dose–response curve. Moreover, systematic errors that stem from the applied treatment technique are smoothed out.

In the study population, the incidence of AVM obliteration is high (obliteration rate 68.2%). The different factors related to such an analysis like follow-up recording, adequate dosimetric data and the different radiobiological models used, make comparisons of data from different sources a complicated task. The retrospective assessment of the treatment outcome and the limitations that such an approach have, are the main source of the lack of data uniformity in radiobiological modelling studies. Furthermore, the quality and the amount of available information in target definition and delineation are usually the limiting factors in the comparison of different studies.

The standard deviations of the fitted parameters were calculated from the whole hyper-surface of the log-likelihood space, as shown in figure 3(b), and not only from a selected plane in the parameter space. This approach is more accurate since the response function used is heavily non-linear and most likely non-symmetric. Figure 3(c) is a qualitative evaluation of the effect that the parameter uncertainties may have in the biological plan analysis, resulting in a dose–response curve accompanied by a confidence interval. Incorporation of the uncertainties characterizing the dose–response curves is important for the introduction of radiobiological modelling in the clinical routine.

The DVHs of the AVM nidus, which were considered to bear the complete dose information since they were calculated from the 3D dose distributions, were used in the calculations of the maximum likelihood fitting. The use of a scalar quantity, such as the mean dose, to quantify AVM obliteration could, of course, simplify the calculations but at the cost of losing much of the structure in the data. The very inhomogeneous dose distributions characterizing AVM stereotactic radiotherapy do not allow this kind of approximation since it is only valid under the hypothesis of having small dose variations. As a consequence of the analysis not only the dose and the irradiated AVM subvolumes, but also the location and the size of the nidus could become key factors in AVM modelling. In the light of these observations the dataset studied could be further analyzed by using a model which would take into account the location of the different partial volumes irradiated.

The patient population was divided into subgroups according to their AVM location (peripheral, central), volume (large, small) and bleeding history (with and without haemorrhage). This division was based on the assumption that location, volume and haemorrhage may have some effect on the radiosensitivity of AVM and consequently on the prescribed dose required to introduce obliteration.

The findings of this study indicate that the percentage incidence of haemorrhage prior radiotherapy increases with the patient's age and the volume of the nidus whereas it is more evident in the centrally located lesions. This conclusion is in accordance with other published studies (Pollock *et al* 1996, Karlsson *et al* 1997a). The influence of factors such as the number of bleeds and certain angioarchitectural features such as morphology (diffuse versus compact), presence of an aneurysm and veinous drainage (superficial or deep) were not examined.

There are reports suggesting that central malformations are more radiosensitive compared to peripherally located AVMs. This is confirmed by this work where although central and peripheral AVMs receive similar doses their obliteration rates differ substantially (77.1% and 62.0% respectively). This is also indicated by their estimated dose–response parameters.

Table 4. Description of the relation of the AVM radiosensitivity with its location and volume. The patient subgroups have been divided into peripheral and central for the location dependence and into large and small using two different cutoffs (2 and 4 cm^3) for the volume dependence. For every subgroup, the clinical obliteration rate and the average biologically effective uniform dose are given. $\bar{\bar{D}}$ was calculated using the parameter estimates $D_{50} = 22.9$ Gy and $\gamma = 1.25$.

Patient subgroups	Large (>2 cm^3) 56.1, 26.1	Small (<2 cm^3) 79.5, 26.0	Large (>4 cm^3) 54.5, 24.5	Small (<4 cm^3) 73.0, 24.6
Peripheral 62.0, 26.4	51.9, 26.7	73.9, 26.1	58.8, 25.6	63.6, 26.9
Central 77.1, 25.5	64.3, 24.9	85.7, 26.0	40.0, 21.4	83.3, 26.4

Note: OR (%), av. $\bar{\bar{D}}$ (Gy)

The proportions of large and small AVMs differ in the two subgroups (small: 46% and 60% respectively), which means that this factor may have some influence on the observed behaviour. This statement is even better described in table 4 where, although in all volume categories the central AVMs receive a lower average $\bar{\bar{D}}$ than the corresponding peripheral AVMs, they show a higher obliteration rate (apart from the case of large (>4 cm^3) where the difference in dose is particularly large, leading to a lower obliteration rate for the central AVMs). The present analysis also suggests that smaller AVMs are more radiosensitive than the large ones, which need more dose to obliterate. The irradiation protocol that was applied during SRT recommended lower dose to large AVMs in order to avoid or reduce possible brain radiation complications. This approach is very well illustrated by the difference in dose that AVMs of different size receive. The irradiation protocol does not apply different prescribed doses according to the bleeding history. The difference in dose between the haemorrhage subgroups observed stems from the proportions of large and small AVMs comprising them.

When using 2 cm^3 as a threshold that separates the large from the small AVMs the corresponding obliteration rates are 56.1% and 79.5% though in the case of the 4 cm^3 threshold the obliteration rates become 54.5% and 73.0% respectively. The dose to the two AVM groups does not differ very much, especially in the first grouping, to reason such a big difference in the obliteration rates. The proportions of central and peripheral AVMs in the two subgroups are comparable in the 2 cm^3 grouping. So, it cannot be argued that the increased radiosensitivity of the small AVMs stems from the central ones. In table 4, it is shown that in all volume and location categories the small AVMs show higher obliteration rates than the corresponding large AVMs even though they receive similar (sometimes even lower) average $\bar{\bar{D}}$ compared to the large AVMs. This statement contradicts the results of other authors (Karlsson *et al* 1999). The Karlsson–Lax model has a trend of underestimating the probability of obliteration for AVMs with a central location and small volume. This analysis supports the speculation that the increased obliteration rate can be dependent on higher venous pressure in central locations, which may result in a lower pressure gradient. It is possible that angioarchitecture factors may have an influence on the probability of obliteration and relatively fewer vessels may need to thrombose to reduce the flow to the critical value at which the obliteration process spontaneously continues, resulting in total obliteration (Meder *et al* 1997).

5. Conclusions

The derivation of the biological parameters D_{50} and γ was performed by using a maximum likelihood fitting. The best values and the confidence intervals of D_{50} and γ were estimated

for the whole patient material as well as for the different patient subgroups (divided according to AVM location, haemorrhage history and volume). In these calculations the AVM volume of 3.0 cm^3 was used as a reference volume and corresponds to the mean value of AVM volume of the study population. Symptoms like epilepsy and/or neurological deficit were not considered relevant to the treatment outcome of obliteration.

The present dataset, consisting of individual AVM obliteration data and individual DVHs for 85 patients irradiated for AVM, could be fitted by the linear Poisson and Karlsson–Lax models. The dose–response curves obtained show that the probability of inducing obliteration of the AVM nidus after radiotherapy depends on the location and the size of the AVM. The uncertainties of the model parameters were quantified from the hyper-surface of the parameter space and were proved to have considerable influence on the dose–response curve. The sets of parameters determined for the two models in the present analysis were used to illustrate the clinical utility of the biological modelling and to estimate their clinical accuracy. Separate dose–response curves were obtained for the different patient subgroups to show the influence of location and volume on AVM radiosensitivity.

For a clinically relevant evaluation of a treatment plan, the use of radiobiological modelling can be very beneficial. The radiobiological evaluation of dose plans can take into account inter-patient radiosensitivity variations allowing a fairly accurate prediction of radiation-induced AVM obliteration. These variations are partly expressed through the confidence intervals calculated during the study. The radiobiological parameters derived are closely associated with the dose delivered to the AVM nidus. These parameters incorporate into the treatment plan evaluation the biological (clinical) information, which is needed to relate the dose delivered to a patient with the clinical findings that follow. Moreover, studies associating the peripheral dose to the AVM nidus and the AVM nidus delineation with the corresponding obliteration rates could prove to be very useful.

Acknowledgments

This research was supported by grants from Cancerföreningen i Stockholm, Konung Gustav V's Jubileumfond; the Research Center for Radiation Therapy; the Center of Excellence of the Swedish National Board for Industrial and Technical Development; TMR, Marie Curie Research Training Grant (Contr No ERBFMBICT).

References

Ågren A K 1995 Quantification of the response of heterogeneous tumors and organized normal tissues to fractionated radiotherapy *PhD Thesis* University of Stockholm, Sweden

Brahme A 1994 Which parameters of the dose distribution are best related to the radiation response of tumours and normal tissues *Proc. Interregional Seminars for Europe, the Middle East and Africa (organized by the IAEA Leuven)* pp 37–58

Brahme A 1995 Treatment optimization using physical and biological objective functions *Radiation Therapy Physics* ed A Smith (Berlin: Springer) pp 209–46

Brahme A 1997 The need for accurate target and dose specifications in conventional and conformal radiation therapy—An introduction *Acta Oncol.* **36** 789–92

Betti O, Munari C and Rossler R 1989 Stereotactic radiosurgery with the linear accelerator: treatment of arteriovenous malformations *Neurosurgery* **24** 311–21

Colombo F *et al* 1994 Linear accelerator radiosurgery for cerebral arteriovenous malformations. An update *Neurosurgery* **34** 14–21

Dutreix J, Tubiana M and Dutreix A 1988 An approach to the interpretation of clinical data on the tumor control probability–dose relationship *Radiother. Oncol.* **11** 239–48

Eadie W T, Drijard D, James F E, Roos M and Sadoulet B 1971 *Statistical Methods in Experimental Physics (CERN)* (Amsterdam: North-Holland)

Emami B, Lyman J, Brown A, Coia L, Goitein M, Munzenrider J E, Shank B, Solin L J and Wesson A M 1991 Tolerance of normal tissue to therapeutic irradiation *Int. J. Radiat. Oncol. Biol. Phys.* **21** 109–22

Flickinger J 1989 The integrated logistic formula and prediction of complications from radiosurgery *Int. J. Radiat. Oncol. Biol. Phys.* **17** 879–85

Flickinger J C *et al* 1996 A dose–response analysis of arteriovenous malformation obliteration after radiosurgery *Int. J. Radiat. Oncol. Biol. Phys.* **36** 873–9

Friedman W, Bova F and Mendenhall W 1995 Linear accelerator radiosurgery for arteriovenous malformations: the relationships of size to outcome *J. Neurosurg.* **82** 180–9

Hladky J P *et al* 1997 Linac stereotactic radiosurgery in AVMs: analysis of a series of 181 patients (abstr.) *XIIth Meeting World Soc. Stereot. Funct. Neurosurg. (Lyon France) Stereotac. Func. Neurosurg.* **67** 95

Jackson A *et al* 1995 Analysis of clinical complication data for radiation hepatitis using a parallel architecture model *Int. J. Radiat. Oncol. Biol. Phys.* **31** 883–91

Källman P, Ågren A K and Brahme A 1992 Tumor and normal tissue responses to fractionated non uniform dose delivery *Int. J. Radiat. Biol.* **62** 249–62

Karlsson B 1996 Gamma Knife surgery of cerebral arteriovenous malformations *PhD Thesis* University of Stockholm, Sweden

Karlsson B, Lax I and Söderman M 1997a Factors influencing the risk of complications following gamma knife radiosurgery of cerebral arteriovenous malformations *Radiother. Oncol.* **43** 275–80

Karlsson B, Lindquist C, Johansson A and Steiner L 1997b Annual risk for the first hemorrhage from untreated cerebral arteriovenous malformations *Neurosurgery* **40** 40–6

Karlsson B, Lindquist C and Steiner L 1997c Prediction of obliteration after Gamma Knife surgery for cerebral arteriovenous malformations *Neurosurgery* **40** 425–31

Karlsson B, Lax I and Söderman M 1999 Can the probability for obliteration after radiosurgery for arteriovenous malformations be accurately predicted? *Int. J. Radiat. Oncol. Biol. Phys.* **43** 313–9

Lax I and Karlsson B 1996 Prediction of complications in gamma knife radiosurgery of arteriovenous malformations *Acta Oncol.* **35** 49–55

Lefkopoulos D, Schlienger M and Touboul E 1993 A 3-D radiosurgical methodology for complex arteriovenous malformations *Radiother. Oncol.* **2** 233–40

Lefkopoulos D, Schlienger M, Merienne L, Levrier M and Touboul E 1994a The associated targets methodology and the multi-isocenters radiosurgery treatment planning system ARTEMIS-3D *Bull. Cancer Radiother.* **81** 111–25

Lefkopoulos D, Schlienger M, Touboul E, Plazas M C and Merienne L 1994b 3-D dosimetric methodology in multiple isocenters radiosurgery: the influence of dose-volume histograms on the choice of the reference isodose *Med. Biol. Eng. Comput.* **32** 440–6

Lind B K, Mavroidis P, Hyödynmaa S and Kappas C 1999 Optimization of the dose level for a given treatment plan to maximize the complication free tumor cure *Acta Oncol.* **38** 787–98

Mavroidis P, Kappas C and Lind B K 1997 A computer program for evaluating the probability of complication-free tumor control incorporated in a commercial treatment planning system *J. Balcan Union Oncol.* **3** 257–64

Mavroidis P *et al* 2000 Comparison of conformal radiation therapy techniques within the dynamic radiotherapy project 'Dynarad' *Phys. Med. Biol.* **45** 2459–81

Mavroidis P, Lind B K and Brahme A 2001 Biologically effective uniform dose ($\bar{D}$) for specification, report and comparison of dose response relations and treatment plans *Phys. Med. Biol.* **46** 2607–30

Meder J F, Oppenheim C, Blustajn J, Nataf F, Lefkopoulos D, Laurent A, Merland J J, Schlienger M and Fredy D 1997 Cerebral arteriovenous malformations: the value of radiologic parameters in predicting response to radiosurgery *Am. J. Neuroradiol.* **18** 1473–83

Merienne L *et al* 1991 Irradiation stéréotaxique de 46 angiomes cérébraux: analyse des résultats angiographiques deux ans et demi après traitement *Neurochirurgie* **37** 185–95

Murtagh B A and Saunders M A 1995 MINOS 5.4 User's Guide *Technical Report* SOL 83–20R Department of Operations Research, Stanford University, Stanford, USA

Niemierko A 1997 Reporting and analysing dose distributions: a concept of equivalent uniform dose *Med. Phys.* **24** 103–10

Pollock B, Kondziolka D, Lunsford L D, Bissonette D and Flickinger J 1996 Factors that predict the bleeding risk of celebral arteriovenous malformations *Stroke* **27** 1–6

Pollock B E *et al* 1998 Factors associated with successful arteriovenous malformations radiosurgery *Neurosurgery* **42** 1239–47

Schilstra C and Meertens H 2001 Calculation of the uncertainty in complication probability for various dose-response models, applied to the parotid gland *Int. J. Radiat. Oncol. Biol. Phys.* **50** 147–58

Schlienger M *et al* 2000 Linac radiosurgery for cerebral arteriovenous malformations: results in 169 patients *Int. J. Radiat. Oncol. Biol. Phys.* **46** 1135–42

Schultheiss T E, Oorton C G and Peck R A 1983 Models in radiotherapy, Volume effects *Med. Phys.* **10** 410–5

Schwartz M *et al* 1997 Prediction of obliteration of arteriovenous malformations after radiosurgery: the obliteration prediction index *Can. J. Neurol Sci.* **24** 106–9

Sisti M B, Kader A and Stein B M 1993 Microsurgery for 67 intracranial arteriovenous malformations less than 3 cm in diameter *J. Neurosurg.* **79** 653–60

Söderman M 2000 Volume determination and predictive models in the management of cerebral arteriovenous malformations *PhD Thesis* University of Stockholm, Sweden

Talairach J and Tournoux P 1992 *Coplanar Stereotaxic Atlas of Human Brain* (Stuttgart: Thieme)

Tew J J, Lewis A I and Reichert K W 1995 Management strategies and surgical techniques for deep-seated supratentorial arteriovenous malformations *Neurosurgery* **36** 1065–72

Theodorou K, Kappas C, Gaboriaud G, Mazal AD, Petrascou O and Rosenwald J C 1997 A simple method for 3D lesion reconstruction from two projected angiographic images: implementation to a stereotactic radiotherapy treatment planning system *Radiother. Oncol.* **43** 281–4

Theodorou K, Rosenwald J C, Siamplis D, Karnabatidis D and Kappas C 1999 A simple method for the correction of distorted digital angiographic images for stereotactic target localization *Cancer Radiother.* **3** 489–93

Touboul E *et al* 1998 Single fraction stereotactic radiotherapy: a dose–response analysis of arteriovenous malformations obliteration *Int. J. Radiat. Oncol. Biol. Phys.* **41** 855-61

Wigg R D 1999 A radiobiological basis for the treatment of arteriovenous malformations *Acta Oncol.* (Suppl 14) **38** 3–29

Withers H R, Taylor J M G and Maciejewski B 1988 Treatment volume and tissue tolerance *Int. J. Radiat. Oncol. Biol. Phys.* **14** 751–9

Yamamoto Y, Coffey R J, Nichols D A and Shaw E G 1995 Interim report on the radiosurgical treatment of cerebral arteriovenous malformations: the influence of size, dose time and technical factors on obliteration rate *J. Neurosurg.* **83** 832–7